



Mesoporous Molecular Sieves Modified with Carbonaceous Deposits*

M. ROZWADOWSKI, M. LEZANSKA AND K. ERDMANN

Faculty of Chemistry, Nicolaus Copernicus University, 87-100 Toruń, Poland

Abstract. There were investigated aluminosilicate MCM-41 samples in the as-prepared form and those modified by the deposition of carbonaceous compounds during conversion of cyclohexene for 12 h. The amount of the deposits decreased with the rising reaction temperature and increased with the Al content of the samples. The cyclohexene conversion followed mainly two mechanisms: cyclohexene skeletal isomerization and hydrogen transfer. The products with 6 carbon atoms in a molecule prevailed in all cases. The process of conversion, proceeding on the Brønsted acid sites, resulted in formation of both coke deposits and volatile products. The creation of coke caused a decrease in the effective concentration of both the Brønsted and the Lewis acid sites. Thermodesorption of pyridine showed that (i) the concentration of these sites before and after the conversion differed only slightly and (ii) the acidic strength of the Brønsted sites was practically independent of their concentration and the sample Si/Al ratio. The chemical composition of the deposits was insignificantly affected by the Al content of the materials and depended mostly on the temperature and duration of the reaction. At relatively low temperatures, both aliphatic and aromatic compounds were formed, being rather weakly bound to the surface of the material. After a longer (55 h) reaction period, some deposits appeared that were strongly bound to the surface. Isotherms of adsorption of water, benzene, and nitrogen were determined, from which a mechanism of this process was derived. It included most probably multilayer adsorption at lower relative pressures, followed by capillary condensation. The sorption capacities of the uncoked samples for benzene and nitrogen were relatively high and independent of the sample Al content. In the case of water, however, an observed reduction in the sorption capacity with the increasing Al content suggested that clusters of the adsorbed molecules formed around the Al centers and caused partial clogging of the material pores. The deposited coke strongly decreased both the surface area and the sorption capacity of the materials.

Keywords: mesoporous molecular sieves, acid sites, conversion of cyclohexene, carbonaceous deposits, adsorption of water, benzene and nitrogen

1. Introduction

Over the past decade, considerable efforts have been made to develop mesoporous materials in order to fill the gap between microporous solids (e.g., zeolites) and mesoporous ones (like oxides and amorphous aluminosilicates). The quest for such materials was initiated mainly by the necessity to obtain acidic catalysts for conversion of hydrocarbons consisted of bulk molecules. The synthesis of the M41S mesoporous molecular sieves of pore diameters within the

1.5–10 nm range became a major breakthrough (Beck et al., 1992; Kresge et al., 1992). MCM-41, a member of the M41S family, exhibits a hexagonal array of cylindrical pores the diameter of which can be controlled. Relatively high thermal stability, specific surface area, and specific pore volume are among the most interesting physical properties of MCM-41 meant as an adsorbent and potential catalyst. When non-modified, the material is catalytically inactive. Active sites may be generated by incorporation of heteroatoms into the electrically neutral, purely siliceous skeleton. Modification of MCM-41 with Al or other (e.g., transition) metals and metal oxides has already been reported

*Dedicated to the memory of Prof. Wolfgang Schirmer.

(Corma et al., 1994; Reddy et al., 1994; Tanev et al., 1994; Sayari et al., 1995a, 1995b, 1995c; Rozwadowski et al., 2000). This modification is a promising way to synthesize materials applicable in catalysis (Sayari et al., 1995c; Sayari, 1996). As the formation of carbonaceous deposits is the main reason for the deactivation of porous zeolite-like catalysts (Deruane, 1985; Bibby et al., 1986; Weitkamp et al., 1986; Karge et al., 1988; Novakova and Kubelkova, 1991), studies on carbonaceous compounds deposited on solid adsorbents are necessary to understand their nature and mechanism of formation.

Previously, we have performed investigations of coked HNaY with a variety of methods, i.e., IR (Rozwadowski et al., 1992a, 1992b; Wloch et al., 1995), UV-Vis (Rozwadowski et al., 1994; Wloch et al., 1995), EPR (Rozwadowski et al., 1994), NMR (Rozwadowski et al., 1994), thermogravimetry (Rozwadowski et al., 1992a, 1992b), and chemical analysis (Wloch et al., 1995). The results have been summarized and discussed elsewhere (Wloch et al., 1998a, 1998b).

In the present paper, we summarize our last results on the formation of carbonaceous deposits during the cyclohexene conversion over Al-MCM-41 as an example of mesoporous molecular sieves of the M41S type. The conversion of cyclohexene has commonly been accepted as a suitable reaction for testing the catalytic behavior of various materials (Cheng and Rajagopalan, 1989; Navio et al., 1996; Radwan and Selim, 1996; Bunjes et al., 1997; Fasi et al., 1997; Navio et al., 1998; Hunka et al., 1999). We have applied this process to characterize the Al-MCM-41 material modified by coking (Rozwadowski et al., 2000), determine the probable mechanism of the respective conversion reaction, describe the active sites, and find a correlation between the postulated mechanism and the nature of the sites (Rozwadowski et al., 2001a, 2001b). Polar (water) and nonpolar (benzene, nitrogen) compounds were chosen as probe molecules for adsorption to learn more about both the lyophilic properties of the examined mesoporous solids and the adsorption process (Rozwadowski et al., 2001c).

2. Experimental

2.1. Materials

The Al-MCM-41 samples were prepared using cetyltrimethylammonium chloride (CTMACl) and

tetraethylammonium hydroxide (TEAOH) as templates included in gel mixtures of the following molar compositions: $\text{SiO}_2:0.17 \text{ CTMACl}:0.4 \text{ TEAOH}:25 \text{ H}_2\text{O}:x \text{ Al}_2\text{O}_3$. Si/Al molar ratios of the gels were chosen to be 15, 30, and 60; thus, x was equal to 0.0333, 0.0167, and 0.0083, respectively.

Proper amounts of aqueous solutions of CTMACl and TEAOH were added to 70% of the total volume of water. Then, 18% of silica was slowly added. The resulting solution was combined with the aluminum compound (aluminum sulfate was added as an aqueous solution and the organic compound as an aqueous suspension). Afterwards, the remaining silica was slowly added and, subsequently, the rest of water was introduced by drops. The resulting blend was stirred for 3 h and then transferred into Teflon-lined autoclaves and heated without stirring at 378 K for 8 days. When cooled down to the room temperature, the product was filtered, washed with water, dried at 373 K, and finally calcined at 773 K.

2.2. Coke Deposition procedure

The cyclohexene conversion was performed at several temperatures between 483 and 663 K (Table 1) in a vertical flow microreactor coupled with a gas chromatograph. The cyclohexene vapor mixed with a carrier gas (5% of C_6H_{10} , 95% of He) was passed at a rate of 0.5 g of C_6H_{10} per hour and gram of the catalyst for 12 h (Rozwadowski, 2001a, 2001d).

2.3. Measurement Techniques

2.3.1. AAS and XRD. The Si/Al ratios of the calcined materials were determined using the atomic absorption spectroscopy (AAS) analysis. X-ray diffraction (XRD) powder patterns were recorded using nickel-filtered CuK_α radiation.

2.3.2. Determination of the Coke Content. The deposit contents of the coked samples were determined as functions of time-on-stream, according to the modified procedure by Bibby and coworkers (Bibby et al., 1986, 1992). 50 mg samples were taken from the reactor at certain time intervals and quickly transferred into weighed glass containers equipped with Teflon stoppers. All the samples were weighed and then calcined in an oxygen flow at 773 K for 5 h. The content of the deposits for an individual sample was obtained from the difference of mass determined before and after

Table 1. Interplanar spacings (d), distances between pore centers (a), BET specific surface areas (S_{BET}), total surface areas (S_t), external surface areas (S_{ext}), surface areas of primary mesopores (S_p), total pore volumes (V_t), external pore volumes (V_{ext}), and primary mesopore volumes (V_p) for the studied Al-MCM-41 materials (Rozwadowski, 2000).

Sample ^a	d (nm)	a^b (nm)	S_{BET} (m ² /g)	S_t (m ² /g)	S_{ext} (m ² /g)	S_p (m ² /g)	V_t (cm ³ /g)	V_{ext} (cm ³ /g)	V_p (cm ³ /g)
Al-MCM-41(15)	4.01	4.64	1031	1043	249	793	1.071	0.462	0.609
Al-MCM-41(15)+C483	n.d.	n.d.	n.d.	438	224	214	0.814	0.659	0.155
Al-MCM-41(15)+C513	n.d.	n.d.	n.d.	701	236	465	0.902	0.561	0.341
Al-MCM-41(15)+C543	n.d.	n.d.	n.d.	780	227	553	0.955	0.588	0.367
Al-MCM-41(15)+C573	3.94	4.55	924	768	226	542	0.986	0.635	0.351
Al-MCM-41(15)+C603	n.d.	n.d.	n.d.	847	230	617	0.945	0.526	0.419
Al-MCM-41(15)+C663	n.d.	n.d.	n.d.	853	232	621	1.097	0.661	0.436
Al-MCM-41(30)	3.56	4.11	1177	1163	158	1005	1.092	0.326	0.766
Al-MCM-41(30)+C573	3.68	4.25	1218	1139	183	956	1.162	0.445	0.716
Al-MCM-41(60)	3.35	3.86	1219	1139	128	1011	0.946	0.301	0.645
Al-MCM-41(60)+C573	3.35	3.86	1320	1156	140	1016	0.995	0.344	0.651

^aThe number in parentheses stands for the Si/Al molar ratio of a synthesis gel and the number following C, for the temperature (K) of coke formation. ^b $a = 2/3^{1/2} d$; n.d. = not determined. Note: areas and volumes are related to a gram of the pure MCM material.

calcination. The samples coked for 12 h and calcined afterwards are referred to as regenerated ones.

2.3.3. Analysis of Volatile Products. The volatile products of the conversion were determined with gas chromatography, using a column packed with a mixture of Chromosorb PAW, DC 550 oil (15%), and stearic acid (3%). The light products with 1 or 2 carbon atoms in a molecule were analyzed using a column filled with Chromosorb 102. An additional analysis of the collected reaction products was carried out using a GC-MS apparatus equipped with a fused silica column covered with an 0.25- μm thick HP-5 film (Rozwadowski, 2001d).

2.3.4. IR and UV-Vis. Before the IR spectra were recorded, the samples pressed into wafers were activated in situ at 630 K under vacuum for 1 h and then exposed at 450 K to pyridine (dried over KOH) that was taken in excess in relation to all the acid sites. Then, physisorbed pyridine was removed by evacuation at the same temperature for 30 min. Subsequently, desorption at 570 K under vacuum was performed. The spectra were recorded after the evacuation at both 450 and 570 K. Prior to the activation, the coked samples were heated at 620 K under nitrogen (1 Pa) for 12 h. The contents of carbon remaining after both the heat treatment and the activation of the samples were determined by the elemental analysis (Rozwadowski, 2001b). Diffuse reflectance infrared Fourier transform (DRIFT) spectra

were recorded within the range of 450–3800 cm^{-1} and UV-Vis spectra, at 190–800 nm.

2.3.5. TGA. Thermogravimetric analysis (TGA) was carried out with use of 100 mg samples under both air and helium within the temperature range of 293–1273 K and at a heating rate of 5 K/min. The samples used in these experiments had been purged with helium overnight during cooling down to room temperature after the reaction.

2.3.6. NMR. ¹³C solid-state NMR spectra were recorded at 75.5 MHz, employing cross polarization, high-power proton decoupling, magic angle spinning, and total suppression of sidebands. A contact time of 1 ms, a recycle time of 5 s, and a 7-mm o.d. zirconia rotor spun at 4.5 kHz were used (Rozwadowski, 2001a). ²⁷Al MAS NMR spectra of the original and coked samples were recorded at 78.2 MHz. The samples were placed in a 7-mm o.d. zirconia rotor spun at 7 kHz (Rozwadowski, 2001b). ²⁹Si MAS NMR spectra of the materials were recorded at 59.6 MHz while the samples were spun at 4.5 kHz (Lezanska, 2002). ¹H NMR spectra of carbonaceous deposits dissolved in CD₂Cl₂ were recorded at 200 MHz.

2.3.7. EPR. EPR spectra were recorded using the X-band. The samples were sealed when under air or evacuated at 10^{−4} Torr and 363 K. The microwave frequency was determined with use of an 18 GHz

microwave counter with the precision of 1 kHz (Nowak, 2002).

2.3.8. Adsorption. The adsorption isotherms of water and benzene were determined at 298.2 K, using a vacuum device equipped with a McBain quartz spring balance and MKS Baratron gauges. The samples (ca. 0.1 g) were activated in situ under stationary vacuum of 10^{-3} Pa at 700 and 363 K for the parent and coked materials, respectively, until a constant mass ($\Delta m \leq 10^{-5}$ g within 12 h) was attained. It was assumed that the adsorption equilibrium was reached when the change in mass was lower than 10^{-5} g for at least 12 h under a constant pressure of adsorbate (Rozwadowski, 2001c). The adsorption isotherms of nitrogen were determined with the ASAP 2010 instrument from Micromeritics. The measurements were performed at 77 K in a static mode. Before the measurements, the parent and coked samples were degassed at 700 and 363 K, respectively, all for at least 8 h and under vacuum of less than 0.7 Pa (Rozwadowski, 2001c).

3. Results and Discussion

3.1. Structural Properties of the Materials

As found with AAS, the Si/Al molar ratios of the calcined products were 12.2, 19.9, and 36.8 for

Al-MCM-41(15), Al-MCM-41(30), and Al-MCM-41(60), respectively.

Figure 1 shows the XRD powder patterns of the parent, coked at 573 K, and regenerated Al-MCM-41 samples. It is evident from the figure that both the coking procedure and the subsequent calcination did not significantly affect the material structure. However, the larger the aluminum content, the inferior the sample quality, as reflected by the shape of the XRD peaks. The patterns enabled to calculate distances between pore centers, which were found to vary over the range of 3.86–4.64 nm and to grow with the Al content of the samples (Table 1).

Other structure parameters of the examined samples, presented in Table 1, were derived from the isotherms of nitrogen adsorption (see Section 3.4). The BET specific surface area, S_{BET} , was calculated using the standard Brunauer-Emmet-Teller method. The total surface area, S_t , the external surface area, S_{ext} , and the primary mesopore volume, V_p , were obtained using the high-resolution α_s -plot method (Gregg and Sing, 1982; Kruk et al., 1997; Sayari et al., 1997) and LiChrospher Si-1000 silica gel ($S_{\text{BET}} = 25 \text{ m}^2/\text{g}$) as a reference adsorbent (Kruk et al., 1997). The S_t value was calculated from the slope of the initial part of the α_s plot (for the samples examined, the initial part of the plot was linear and passed the origin of the co-ordinate system). S_{ext} and V_p were calculated from the slope of a linear part of the α_s plot over the range between the

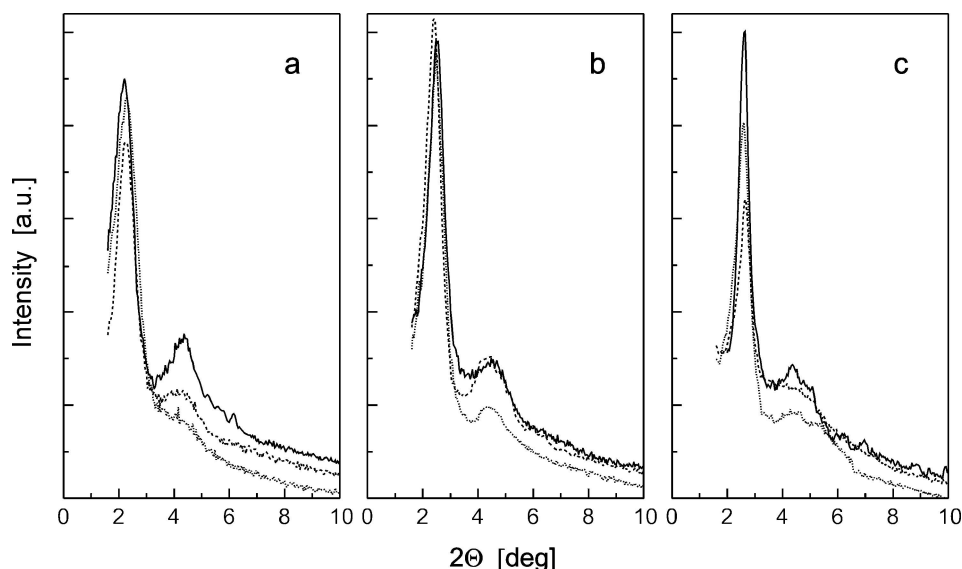


Figure 1. XRD powder patterns of Al-MCM-41(15) (a), Al-MCM-41(30) (b), and Al-MCM-41(60) (c). Solid, dashed and dotted lines correspond to the parent, coked at 573 K, and regenerated samples, respectively (Rozwadowski, 2000).

pressure corresponding to the termination of nitrogen condensation in the primary mesopores and that associated with the onset of capillary condensation in the secondary mesopores and in macropores (Kruk et al., 1997). The total surface area of the material was assumed to be the combined surface area of all mesopores and macropores. The external surface area was considered to be that of the macropores and the secondary mesopores together. The surface area of the primary mesopores, S_p , was simply equal to the difference $S_t - S_{ext}$. The total pore volume, V_t , was determined from a single-point adsorption at the relative pressure of 0.99 by converting the volume of the adsorbed gaseous nitrogen to the volume of liquid nitrogen. The combined volume of the macropores and the secondary mesopores, V_{ext} , was equal to $V_t - V_p$. The results of the calculations made with the α_s -plot method did not indicate formation of a significant number of micropores in any coked sample.

The Barrett-Joyner-Halenga (BJH) method (Barrett et al., 1951) was employed to calculate the average pore size and pore size distribution from the nitrogen desorption data (Fig. 2). For that purpose, a relation was used in which a correction for the thickness of a statistical film present on the surface of pore walls was added to the Kelvin equation (Kruk et al., 1997; Maglara et al., 1997). More details can be found elsewhere (Rozwadowski, 2000).

The BET specific surface area and the primary mesopore volume for the coked Al-MCM-41(15) clearly differed from the respective values for the parent sample (Table 1). For Al-MCM-41(30) and Al-MCM-41(60), however, the differences in S_{BET} and V_p were much smaller. These results suggested that deposition of coke proceeded mostly in the aluminum-rich pores. The coking could then be considered as the process sensitive to both the reaction temperature and the aluminum content of the material. Noteworthy was that the examined samples exhibited no or only small changes in the interplanar spacing upon coking (Table 1).

As expected, modification of Al-MCM-41 by the deposition of coke under various conditions yielded materials exhibiting reduced volume and surface area of pores.

3.2. Catalytical Centers of the Materials

The conversion of cyclohexene over the studied materials proved the presence of strong Brønsted acid sites. As found for Al-MCM-41(15), the conversion increased with the reaction temperature (Rozwadowski, 2001b). It was relatively low (ca. 52%) at 483 K, then it increased rapidly to ca. 96% at 543 K, and finally remained practically constant up to 663 K. The reaction yield increased with the Al content of the catalysts,

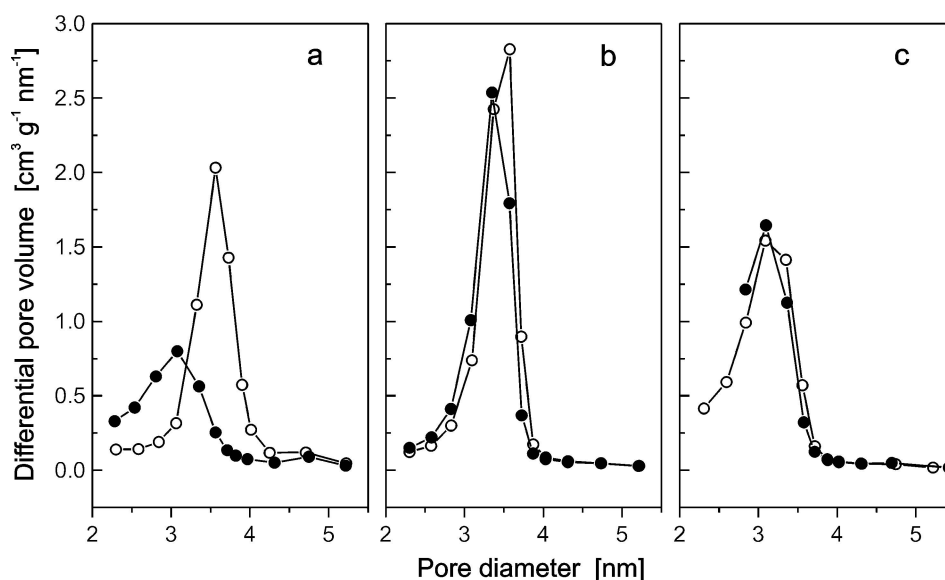


Figure 2. BJH pore size distributions obtained from nitrogen desorption for the parent samples (open circles) and samples coked at 573 K (full circles) of (a) Al-MCM-41(15), (b) Al-MCM-41(30), and (c) Al-MCM-41(60). The volumes are normalized to a gram of the pure MCM material (Rozwadowski, 2000).

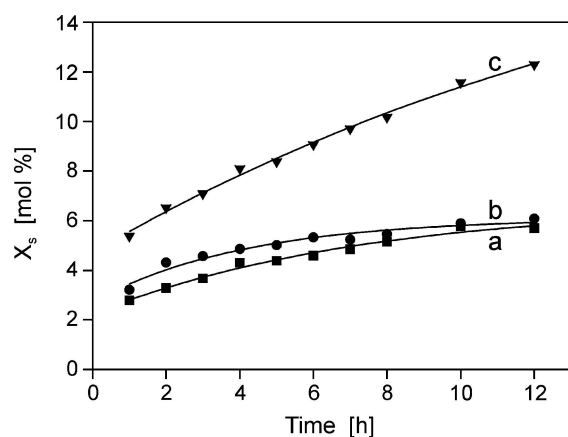


Figure 3. Fractions of unreacted substrate (X_s) after cyclohexene conversion at 573 K over (a) Al-MCM-41(15), (b) Al-MCM-41(30), and (c) Al-MCM-41(60) vs. reaction time (Rozwadowski, 2001b).

which was seen from the decreasing amount of unreacted cyclohexene (Fig. 3). The catalytic activity decreased slightly with the reaction time for Al-MCM-41(15) and Al-MCM-41(30) and markedly for Al-MCM-41(60) (Fig. 3).

The occurrence of the Brønsted and Lewis acid sites in the catalysts has been confirmed by the IR spectra in the range of OH group vibrations. The spectrum of the original Al-MCM-41(30) sample (Fig. 4(a)) showed a clear band at 3740 cm^{-1} , typical of silanol OH groups as well as of acidic hydroxyls in Al-MCM-41 and in amorphous aluminosilicates (Weglarski, 1996). The deposition of carbonaceous compounds caused a reduction in intensity of this band due to the van der Waals interactions between hydroxyls and coke (Fig. 4(b)).

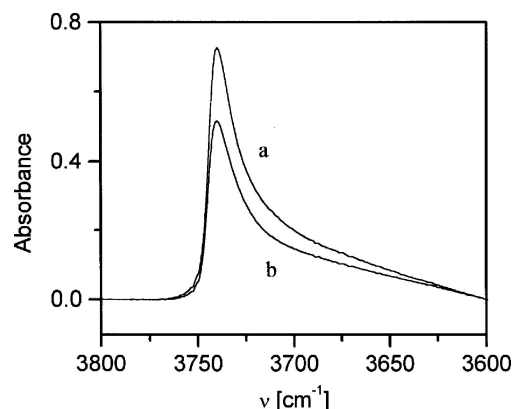


Figure 4. IR spectra of OH groups in (a) original and (b) coked Al-MCM-41(30), activated at 630 K (Rozwadowski, 2001b).

The IR bands at 1455 and 1545 cm^{-1} , assigned to pyridine molecules bound to the Lewis sites (PyL) and to pyridinium ions associated with the Brønsted sites (HPy^+), respectively, allowed for calculation of the acid site concentrations. The relevant extinction coefficients were derived from the spectra of pyridine adsorbed on both zeolite HY and dehydroxylated zeolite HY, containing almost exclusively the Brønsted and Lewis acid sites, respectively (Cerqueira, 2000a, 2000b). The acidic strength of the Brønsted sites was estimated from the temperature-programmed desorption (TPD) of pyridine at 570 K.

As found, the concentrations of the Brønsted and Lewis acid sites (Table 2) increased with the Al content and were twice as high in Al-MCM-41(30) with $\text{Si/Al} = 19.9$ as in Al-MCM-41(60) with $\text{Si/Al} = 36.8$ whereas they were only slightly higher in

Table 2. Concentrations and acidic strength of Brønsted and Lewis acid sites in original and coked Al-MCM-41(n) (Rozwadowski, 2001b).

Sample	<i>n</i>	Content of carbon ^a (wt%)	Brønsted sites ($\mu\text{mol g}^{-1}$)	Lewis sites ($\mu\text{mol g}^{-1}$)	Acidic strength of Brønsted sites A_{des}/A_0
Original	15	n.a.	157	527	0.53
	30	n.a.	147	473	0.64
	60	n.a.	88	211	0.69
Coked	15	3.7	152	520	0.52
	30	5.7	123	425	0.62
	60	6.1	61	198	0.56

^aThe samples were coked at 573 K; prior to the IR measurements, they were thermally treated at 620 K under nitrogen (1 Pa) for 12 h and subsequently activated at 630 K under vacuum for 1 h. A_0 and A_{des} are the intensities of the HPy^+ band in the FTIR spectra, corresponding to the samples subjected to the evacuation at 450 K and desorption at 570 K, respectively. n.a. means not applicable.

Al-MCM-41(15) with Si/Al = 12.2 than in Al-MCM-41(30). Probably, a fraction of Al atoms in the sample of the largest Al content formed clusters that created neither Brønsted nor Lewis sites.

The deposition of coke caused a minor reduction in the concentrations of both the Brønsted and Lewis sites (Table 2). The smallest effect was observed for Al-MCM-41(15) that contained the lowest amount of coke remaining after the thermal treatment. A decrease in the concentration of the Brønsted sites upon coking was observed also by others (Cerqueira, 2000a, 2000b) in the case of coked dealuminated HY zeolites, but, as opposed to Al-MCM-41, the formation of comparable amount of coke did not influence the properties of the Lewis sites in HY. The results of TPD of pyridine suggested that carbonaceous deposits practically did not influence the acidic strength of the Brønsted sites. The relatively small differences between the acid site concentrations determined before and after the conversion of cyclohexene proved that pyridine could penetrate to the acid centers in spite of blocking the surface by the deposits. The extent of this diffusion depended presumably on the coke composition. The thermal treatment of the coked samples at 620 K under nitrogen and subsequent activation at 630 K under vacuum might contribute to a further partial removal of the coke deposits from the examined samples.

The deposition of coke caused changes in the ratio of tetrahedral to octahedral aluminum in the samples (Fig. 5). A slight increase in this ratio upon coking was observed for the sample with the largest total content of aluminum, which might result from a repeated introduction of Al into the skeleton. A reduced fraction of the tetrahedral aluminum was found for the sample with the least total content of aluminum, which might be caused by a partial dealumination and a decrease in the degree of order in the vicinity of aluminum tetrahedra. This was proved (Lezanska, 2002) by the presence of single broad bands in the ^{29}Si MAS NMR spectra of the coked Al-MCM-41 samples while three well resolved and slightly less resolved lines were observed for uncoked Al-MCM-41(60) and Al-MCM-41(30), respectively (Fig. 6). The spectrum for the uncoked Al-MCM-41(15) sample was poorly resolved because of a relatively large concentration of Al.

3.3. Cyclohexene Conversion Products

Analysis of the volatile products of the cyclohexene conversion over Al-MCM-41 allowed one to conclude

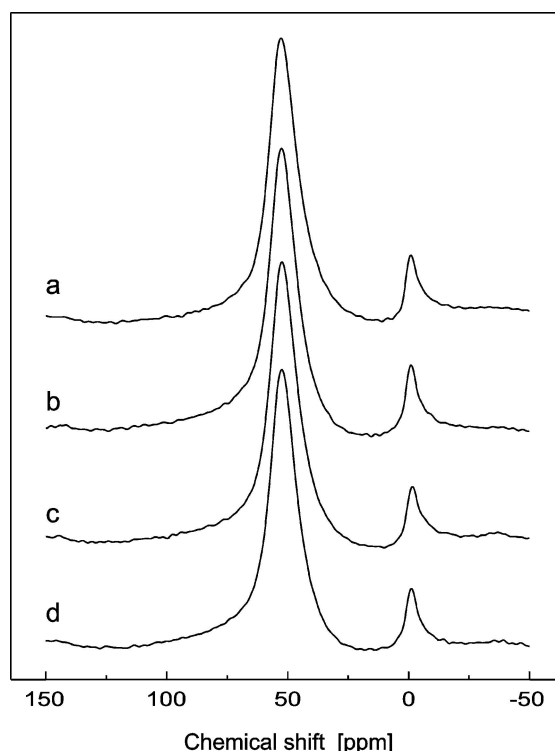


Figure 5. ^{27}Al MAS NMR spectra of Al-MCM-41(15) samples: a – original; b, c, and d – coked at 513, 573, and 663 K, respectively (Rozwadowski, 2001b).

as follows. Cyclohexene skeletal isomerization (CSI) and hydrogen transfer (HT) were the main reactions involved in this process (Rozwadowski, 2001d). Among various hydrocarbons formed in the reactions of CSI, HT, and cracking, the compounds containing 6 carbon atoms in a molecule predominated, independently of the conditions of the process. For temperatures below 603 K, a high selectivity of the studied materials to the C_6 compounds was observed, which still increased with the reaction time. It was probably caused by the fact that the strongest acid sites of the catalysts, responsible for cracking, became deactivated first of all and then those associated with alkylation.

The catalyst deactivation was determined by both the amount of deposits and the ratio of 1-methylcyclopentane (MCPA) to 1-methylcyclopentene (1-MCPE), increasing with the reaction time (Rozwadowski, 2001d). The change in selectivity with the reaction time might result from a secondary reaction, in which 1-MCPE became converted into MCPA over coke. It was accompanied by a reduction in the hydrogen content of the coke and, at the same time, by enrichment in hydrogen of the volatile products,

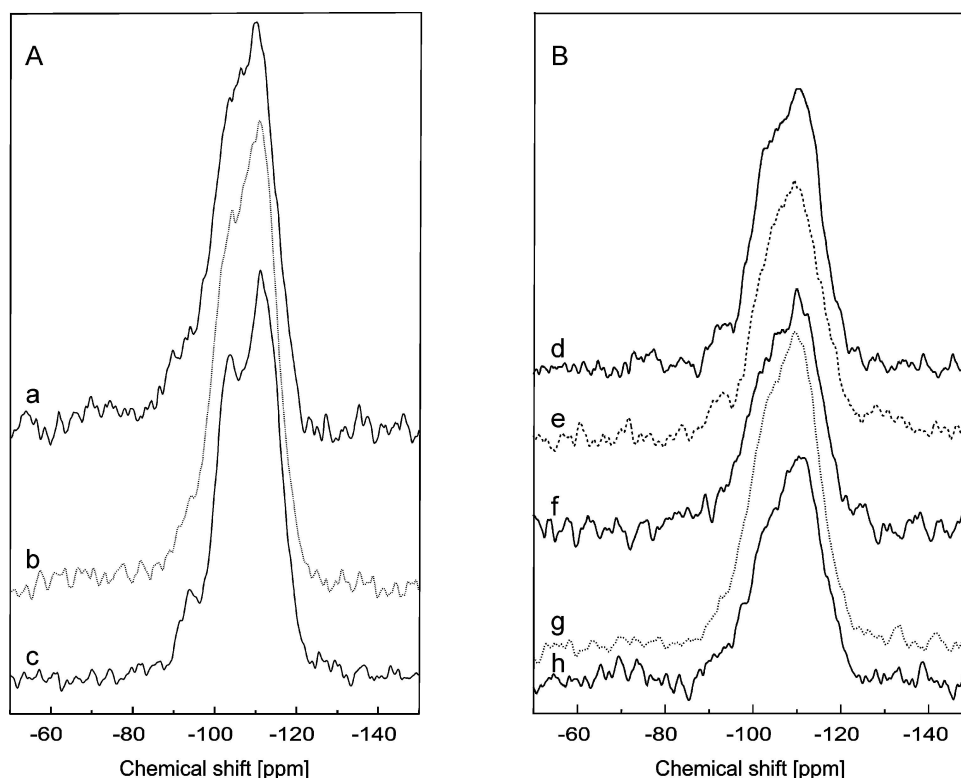


Figure 6. ^{29}Si MAS NMR spectra of original (A) and coked (B) samples of (a) Al-MCM-41(15), (b) Al-MCM-41(30), (c) Al-MCM-41(60), (d) Al-MCM-41(60)+C573, (e) Al-MCM-41(30)+C573, (f) Al-MCM-41(15)+C513, (g) Al-MCM-41(15)+C573, and (h) Al-MCM-41(15)+C663 (Lezanska, 2002).

the latter process being indicated by an increase in the contribution of MCPA (Rozwadowski, 2001d).

Investigation of the carbonaceous deposits with the spectroscopic methods (EPR, IR, and UV-Vis) allowed one to draw further conclusions. The EPR spectra revealed an increase in the spin concentration with the coking temperature rising from 483 to 513 K, which was associated with an increasing number of free-radical structures (Nowak, 2002). A similar increase in the spin concentration was observed after a longer reaction time (55 h), which suggested that under these conditions the deposits formed multilayer polyaromatic structures strongly bound to the surface.

The FTIR spectra of the carbonaceous deposits indicated that branching of the aliphatic substituents decreased with the rising reaction temperature (Fig. 7). Superposition of the bands assigned to vibrations of the C=C bonds in alkenes and aromatics made interpretation of the spectra difficult to some extent. However, differences in the band intensities within the short-wave regions of the spectra (C-H stretching vibration range), occurring upon a change in the reaction temperature, in-

dicated formation of paraffinic and olefinic compounds at the lower temperatures and of aromatic and some olefinic compounds at the higher ones (Rozwadowski, 2001a). This conclusion was confirmed by a shift of the band at 1600 cm^{-1} to 1590 cm^{-1} with the rise of the reaction temperature, associated probably with delocalization of the π bond. The same applies to the band at 1495 cm^{-1} that shifted to 1510 cm^{-1} .

The UV-Vis spectra (Fig. 8) indicated that diene structures (acyclic coupled dienes and cyclic dienes) as well as aromatic ones were present in the coke (Rozwadowski, 2001a). The spectra confirmed that Al-MCM-41(30) and Al-MCM-41(60) contained less coke as compared to Al-MCM-41(15) and the deposits present in the latter sample included less olefinic compounds.

The chemical composition of coke (Table 3) showed that the hydrogen contribution to the carbonaceous deposits decreased with the increasing reaction temperature (Lezanska, 2002). The lowest C/H ratios, 0.89 and 0.93, were found for the deposits formed at 483 and 513 K, respectively. They indicated the deposits of an

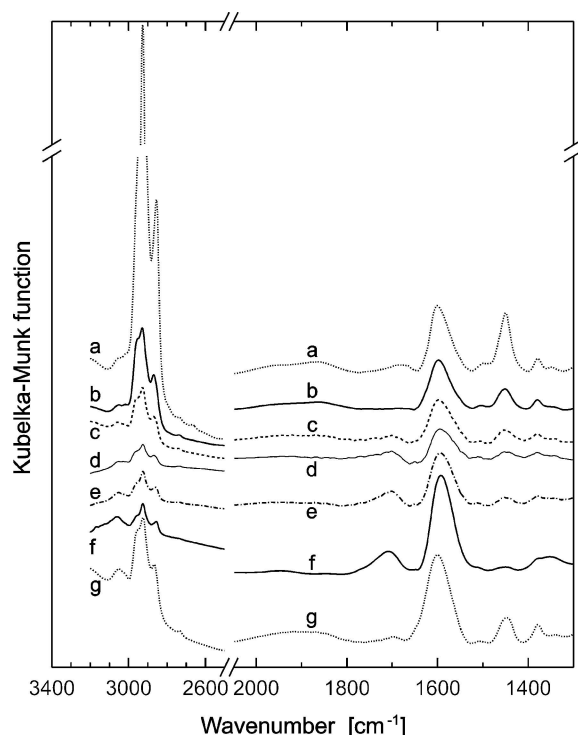


Figure 7. DRIFT spectra of Al-MCM-41(15) after the reactions at (a) 483, (b) 513, (c) 543, (d) 573, (e) 633 and (f) 663 K for 12 h, and (g) after the reaction at 573 K for 55 h (Rozwadowski, 2001a).

olefinic character, e.g., hydrocarbon chains with alternating single and double bonds. The deposits formed at these two temperatures were totally soluble in CH_2Cl_2 and similar to each other as it resulted from the FTIR investigations (Lezanska, 2002). Starting from 543 K, carbonaceous compounds insoluble in CH_2Cl_2 appeared in the coke. The insoluble fraction varied from ca. 30 to 92% when the reaction temperature increased from 543 to 663 K. The C/H values of the coke indicated that the soluble deposits, formed below and above 543 K, included carbonaceous compounds of a similar character. Elongation of the coking time from 12 to 55 h did not influence the C/H ratio for the soluble deposits that constituted in this case ca. 50% of the total coke. The ratios of numbers of aliphatic to aromatic protons for the soluble deposits, obtained from ^1H NMR (Table 3), demonstrated an increase in aromaticity of these deposits with the reaction temperature rising up to 603 K and then a decrease for the higher temperatures, which was confirmed by the IR investigations (Lezanska, 2002). Presumably, the deposits formed at temperatures above 603 K were mainly polyaromatic and a small fraction, soluble in CH_2Cl_2 , contained

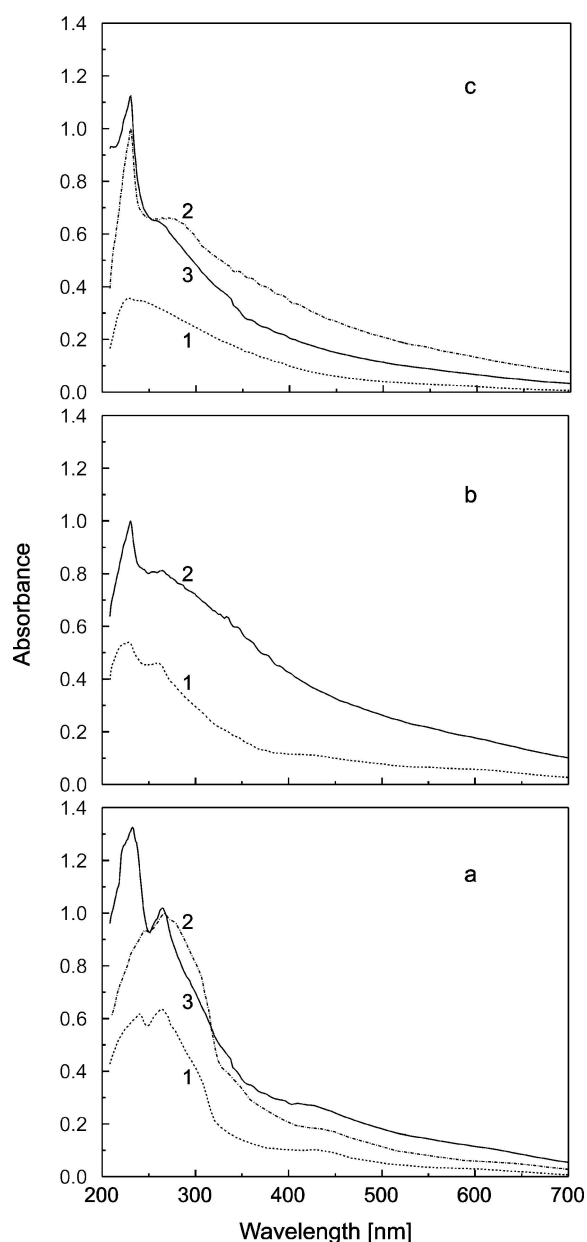


Figure 8. UV-Vis spectra of Al-MCM-41(15) after the reactions at (a) 483, (b) 573, and (c) 663 K for (1) 4 h, (2) 12 h, and (3) 12 h with successive purging with helium during cooling to room temperature overnight (Rozwadowski, 2001a).

mostly aliphatic compounds. The thermogravimetric analysis confirmed these conclusions (Fig. 9): intensity of the high-temperature peak of the DTA curve increased with the coking temperature (Rozwadowski, 2001a).

The IR investigations of the soluble deposits showed that differences between aliphatic substituents

Table 3. Characteristics of carbonaceous deposits formed on Al-MCM-41 materials during cyclohexene conversion at various temperatures for 12 h (Lezanska, 2002).

Sample ^a	Total coke content (%)	Fraction of coke soluble in CH ₂ Cl ₂ (%)	C/H		Weighted average
			Coke insoluble in CH ₂ Cl ₂	Coke soluble in CH ₂ Cl ₂	
Al-MCM-41(15)+C573	28.38	13.46	1.18	0.81	1.02
Al-MCM-41(30)+C573	13.54	9.16	1.32	0.90	1.05
Al-MCM-41(60)+C573	6.92	4.42	1.26	1.10	1.16
Al-MCM-41(15)+C663	13.46	1.28	1.26	0.84	1.22
Al-MCM-41(15)+C633	21.12	0.64	1.27	0.46	1.24
Al-MCM-41(15)+C603	18.85	4.85	1.21	1.03	1.17
Al-MCM-41(15)+C573	28.38	13.46	1.18	0.81	1.02
Al-MCM-41(15)+C543	23.24	19.74	1.22	0.86	0.92
Al-MCM-41(15)+C513	33.80	33.90	n.d.	0.93	0.93
Al-MCM-41(15)+C483	48.81	48.80	n.d.	0.89	0.89
Al-MCM-41(15)+C573 ^b	60.17	36.81	1.42	0.81	1.10

^aSample designation as in Table 1. ^bDuration of the reaction: 55 h. n.d. = not determined.

formed at temperatures rising up to 573 K decreased (Lezanska, 2002). The deposits formed at the two lowest and two highest temperatures consisted of mostly aliphatic and alkyl-aromatic compounds, respectively. The extent of substituent branching, obtained from the contributions of CH₂ and CH₃ groups, decreased with the coking temperature rising up to 573 K. In the deposits formed at the higher temperatures, the branched substituents were probably connected directly to aromatic rings.

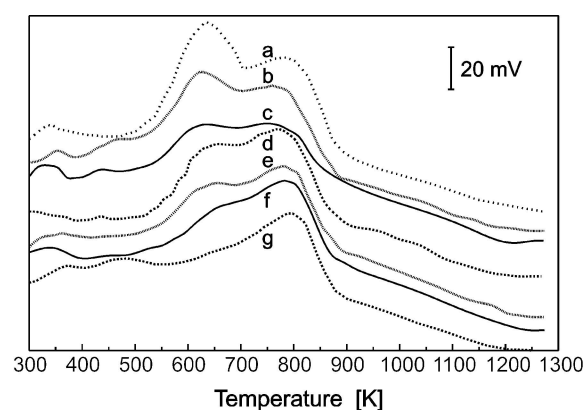


Figure 9. DTA plots for Al-MCM-41(15) after the reactions at (a) 483, (b) 513, (c) 543, (d) 573, (e) 603, (f) 633, and (g) 663 K for 12 h. Analyses under air (Rozwadowski, 2001a).

3.4. Sorption Properties of the Materials

Adsorption of polar (water) and nonpolar (benzene and nitrogen) compounds on the studied materials was carried out to study the adsorption mechanisms and porous structure of the adsorbents. Investigation of the total sorption capacities and isotherm steps for the particular samples and adsorbates gave interesting results (Rozwadowski, 2001c).

Apparently, the most unexpected features were found for water. The sorption capacities of both the parent and coked samples followed the sequence Al-MCM-41(15) < Al-MCM-41(60) ≤ Al-MCM-41(30), i.e., higher values were found for samples with smaller amounts of the Al centers (Fig. 10, Table 4). It might be expected that adsorption of water should be higher for the samples with a larger amount of the Al centers located in the much less hydrophilic silica walls of MCM-41 (Branton, 1995; Llewellyn, 1995). At the same time, the heights of the isotherm steps increased in the same sequence, which meant that the smallest amount of condensed water occurred in the sample with the largest content of Al. Similar relations were observed for the coked samples of various contents of Al (Fig. 10, Table 4). This unexpected behavior could not originate from clogging the pores with some extraframework Al species since, in such a case, the sorption capacities for benzene and

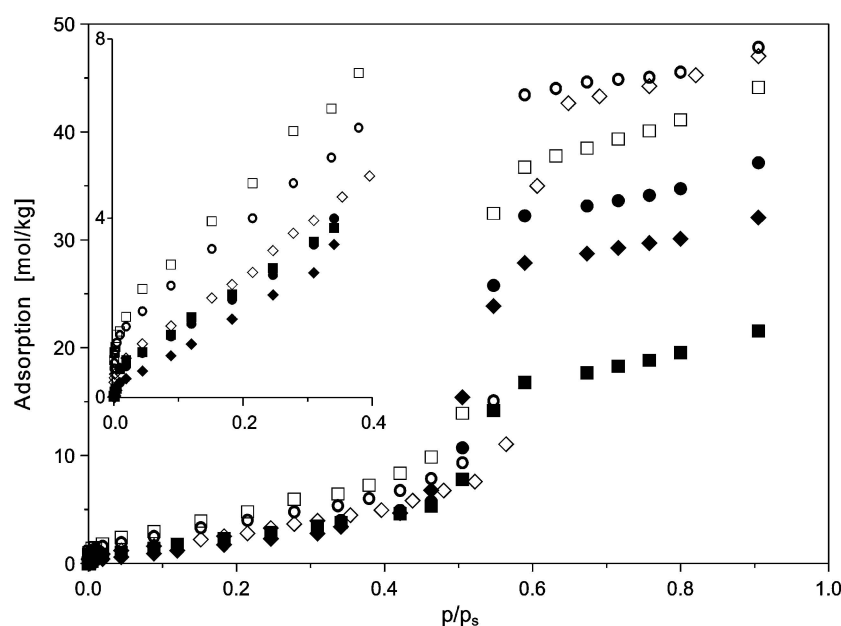


Figure 10. Isotherms of water adsorption on the parent (open symbols) and coked at 573 K (filled symbols) samples of Al-MCM-41(15) (squares), Al-MCM-41(30) (circles), and Al-MCM-41(60) (diamonds) (Rozwadowski, 2001c).

nitrogen could not be higher than that for water (see below).

At the relative pressures above the condensation step, adsorption of water increased relatively little and the isotherms were parallel to one another (Fig. 10). The samples became nearly saturated with water at $p/p_s \cong$

0.6. The same applies to the coked samples of various contents of aluminum (Fig. 10).

The sorption capacities of all the parent and coked samples for benzene (Table 4 and Fig. 11) appeared to be higher than those for water. The relationships between these capacities and both the Al content and the reaction temperature were similar to those for water, which was rather surprising when considering the non-polar character of benzene molecules in comparison to polar water molecules.

The sorption capacities for nitrogen (Fig. 12) were generally close to those for benzene, i.e., also higher than those for water. The only difference was that the capacity of Al-MCM-41(60) was lower not only than that of Al-MCM-41(30) but also lower than that of Al-MCM-41(15). This was accompanied by the least height of the isotherm step for that sample. The other features were the same as those for benzene and water.

The above experimental findings can be explained assuming the following mechanism of adsorption. The polar water molecules are strongly bound to the Al centers present on the pore wall surface. That strong bonding and subsequent association of water molecules lead to formation of liquid-like water clusters around the Al centers and to clogging the pores. Thus, the diffusion of water is hindered and, consequently, water fills the pores only partially, i.e., only the pore fragments

Table 4. Sorption capacities of the parent and coked Al-MCM-41 materials ($p/p_s = 0.85$) (Rozwadowski, 2001c).

Sample ^a	H ₂ O (298.2 K) (cm ³ /g)	C ₆ H ₆ (298.2 K) (cm ³ /g)	N ₂ (77 K) (cm ³ /g)
Al-MCM-41(15)	0.771	0.864	0.850
Al-MCM-41(15)+C483	0.290	0.426	0.278
Al-MCM-41(15)+C513	0.348	0.433	0.423
Al-MCM-41(15)+C543	0.350	0.424	0.473
Al-MCM-41(15)+C573	0.372	0.414	0.441
Al-MCM-41(15)+C603	0.435	0.478	0.537
Al-MCM-41(15)+C663	0.492	0.529	0.580
Al-MCM-41(30)	0.845	0.963	0.922
Al-MCM-41(30)+C573	0.650	0.744	0.788
Al-MCM-41(60)	0.835	0.917	0.771
Al-MCM-41(60)+C573	0.562	0.612	0.737

^aSample designation as in Table 1.

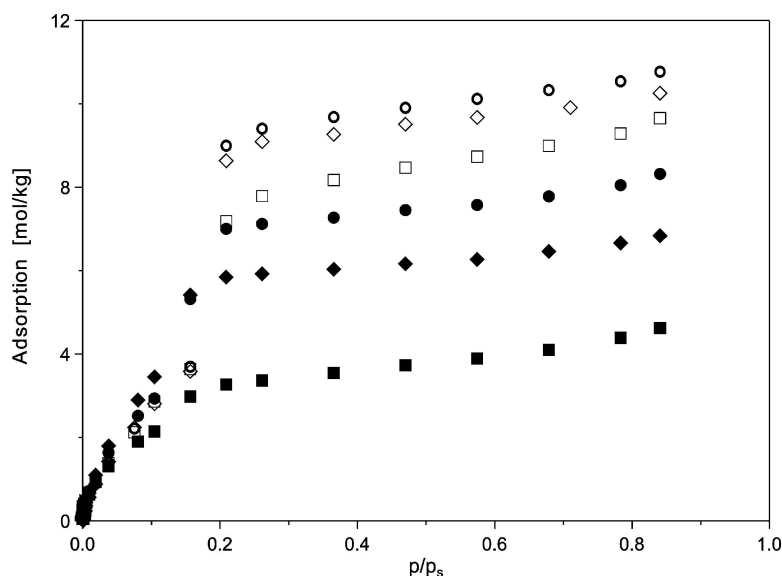


Figure 11. Isotherms of benzene adsorption on the parent (open symbols) and coked at 573 K (filled symbols) samples of Al-MCM-41(15) (squares), Al-MCM-41(30) (circles), and Al-MCM-41(60) (diamonds) (Rozwadowski, 2001c).

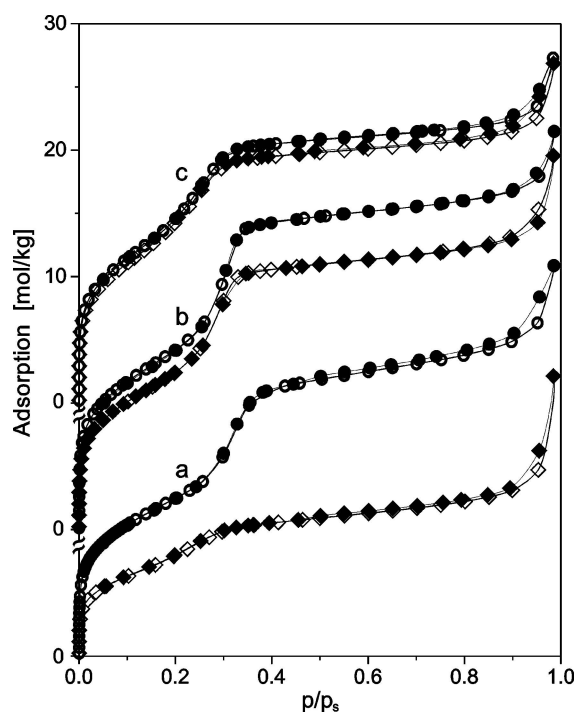


Figure 12. Isotherms of nitrogen adsorption on the parent (circles) and coked at 573 K (diamonds) samples of Al-MCM-41(15) (a), Al-MCM-41(30) (b), and Al-MCM-41(60) (c). Open and filled symbols correspond to adsorption and desorption, respectively (Rozwadowski, 2001c).

near the Al centers. Obviously, this effect should increase with a growing number of the Al centers and with a decreasing distance between the centers as the water clusters can grow larger and be anchored on more Al centers jointly. Such clusters should be more strongly localized and would probably require higher activation energy for a rearrangement. Thus, even larger regions inaccessible to water can be left than in the case of the Al centers separated with longer distances. Such a picture agrees well with the observation that the sorption capacities for nitrogen and benzene are higher than that for water. Nevertheless, a hydrophobic nature of both silica skeleton and coke might also contribute to lowering adsorption of water with respect to that of benzene and nitrogen.

4. Conclusions

- The amounts of carbonaceous deposits formed on the studied Al-MCM-41 molecular sieves during the conversion of cyclohexene decrease with the rising reaction temperature and increase with the amount of aluminum introduced into the materials. Such a modification of the Al-MCM-41 sample with the largest Al content leads to appreciable surface and structural changes, e.g., to a decrease in the specific surface area and pore volume.

- The studied materials differ in the concentrations of the Brønsted and Lewis acid sites, which generally increase with the Al content of the samples up to a limited value. The fact that the cyclohexene conversion occurs over the Al-MCM-41 catalysts indicates that among the Brønsted sites are those of strong acidity.
- The conversion of cyclohexene follows mainly two concurrent mechanisms, i.e., cyclohexene skeletal isomerization and hydrogen transfer, resulting in formation of the C₆ hydrocarbons that predominate in the products under all conditions studied. Cracking and alkylation accompany these two reactions, as indicated by volatile products comprising compounds with 1–5, 7, and 8 carbon atoms. All these processes require the presence of acid sites in the catalysts.
- The deposition of coke causes a decrease in the conversion level, which consequently indicates an apparent reduction in the concentrations of both the Brønsted and the Lewis acid sites or, in other words, a reduction in the effective concentrations. Thermodesorption of pyridine shows relatively small differences between the concentrations before and after the conversion and no difference in the acidic strength of the Brønsted sites. Thus, pyridine seems to be able to penetrate to the acid centers in spite of the blocking of the surface by carbonaceous deposits.
- The chemical nature of the carbonaceous compounds deposited on the studied catalysts depends mainly on the temperature of the reaction. Both aliphatic and aromatic compounds are formed in the process of the cyclohexene conversion. However, the higher the reaction temperature, the larger the content of aromatic deposits. At relatively low temperatures, the deposits remain on the inner surface (i.e., in the pores) of the examined materials. A part of the deposits is rather weakly bound to the surface and gets removed after the reaction when the coked material is purged with helium. Application of a longer reaction time (55 h) leads to formation of some deposits that are either strongly bound to the surface or blocked in the pores and that cannot be removed upon heating even to 1273 K under helium. At higher temperatures, a fraction of the coke migrates out of the pores. Then, this fraction (most probably aliphatics) partially desorbs and moves away, while the other part (presumably aromatics) adsorbs on the external surface of the catalyst.
- Processes of adsorption of water, benzene, and nitrogen on the examined materials conform to

similar mechanisms, including multilayer adsorption at lower relative pressures followed by capillary condensation of an adsorbate. The capillary condensation of adsorbed water occurs at low relative pressures due to interactions with the Al centers. Unexpectedly, an increase in the Al content, i.e., in the number of hydrophilic centers, causes a reduction in the sorption capacity. This is likely due to formation of clusters of liquid water around the Al centers and clogging of the pores. Such a mechanism is supported by the fact that the sorption capacities for benzene and nitrogen (nonpolar compounds) are clearly higher than that for water. However, a hydrophobic nature of both silica skeleton and coke may also contribute to lowering adsorption of water with respect to that of benzene and nitrogen.

Nomenclature

α_s	A type of a plot used for calculating structure parameters of a porous solid
a	Distance between pore centers, nm
A_0	Intensity of the IR band assigned to HPy ⁺ for the sample with the adsorbed pyridine and then evacuated at 450 K, arbitrary units
A_{des}	Intensity of the IR band assigned to HPy ⁺ for the sample with the adsorbed pyridine and then desorbed at 570 K, arbitrary units
C/H	Ratio of the numbers of carbon and hydrogen in coke
CSI	Cyclohexene skeletal isomerization
d	Interplanar spacing, nm
HT	Hydrogen transfer
n	Si/Al ratio of a synthesis gel
p/p_s	Relative pressure of adsorbate
R	Universal gas constant, J mol ⁻¹ K ⁻¹
S_{BET}	BET specific surface area, m ² g ⁻¹
S_{ext}	External surface area, m ² g ⁻¹
S_p	Surface area of primary mesopores, m ² g ⁻¹
S_t	Total surface area, m ² g ⁻¹
V_{ext}	External pore volume, cm ³ g ⁻¹
V_p	Primary mesopore volume, cm ³ g ⁻¹
V_t	Total pore volume, cm ³ g ⁻¹

Acknowledgments

The authors are indebted to Prof. J. Datka (Cracow, Poland) for the IR analysis of acid centers. The work was partially supported by the State Committee for

Scientific Research (KBN) with the grant no. 4 T09A 147 23.

References

- Barett, E.P., L.G. Joyner, and P.P. Halenda, "The Determination of Pore Volume and Area Distributions in Porous Substances. I. Computations from Nitrogen Isotherms," *J. Am. Chem. Soc.*, **73**, 373–380 (1951).
- Beck, J.S., J.C. Vartuli, W.J. Roth, M.E. Leonowicz, C.T. Kresge, K.D. Schmitt, C.T.W. Chu, D.H. Olson, E.W. Sheppard, S.B. McCullen, J.B. Higgins, and J.L. Schlenker, "A New Family of Mesoporous Molecular Sieves Prepared with Liquid Crystal Templates," *J. Am. Chem. Soc.*, **114**, 10834–10843 (1992).
- Bibby, D.M., N.B. Milestone, J.E. Patterson, and L.P. Aldridge, "Coke Formation in Zeolite ZSM-5," *J. Catal.*, **97**, 493–502 (1986).
- Bibby, D.M., R.F. Howe, and G.D. McLellan, "Coke Formation in High-Silica Zeolites," *Appl. Catal.*, **93**, 1–34 (1992).
- Branton, P.J., P.G. Hall, and K.S.W. Sing, "Physisorption of Alcohols and Water Vapor by MCM-41, a Model Adsorbent," *Adsorption*, **1**, 77–82 (1995).
- Bunjes, A., I. Eilks, M. Pahlke, and B. Ralle, "On the Disproportionation of Cyclohexene and Related Compounds," *J. Chem. Ed.*, **74**, 1323–1325 (1997).
- Cerqueira, H.S., P. Ayrault, J. Datka, P. Magnoux, and M. Guisnet, "m-Xylene Transformation over a USHY Zeolite at 523 K and 723 K: Influence of Coke Deposits on Activity, Acidity, and Porosity," *J. Catal.*, **196**, 149–157 (2000a).
- Cerqueira, H.S., P. Ayrault, J. Datka, and M. Guisnet, "Influence of Coke on the Acid Properties of USY Zeolite," *Micropor. Mesopor. Mater.*, **38**, 197–205 (2000b).
- Cheng, W.-C. and K. Rajagopalan, "Conversion of Cyclohexene over Y-Zeolites: a Model Reaction for Hydrogen Transfer," *J. Catal.*, **119**, 354–358 (1989).
- Corra, A., M.T. Navarro, and J. Perez-Pariente, "Synthesis of Ultralarge Pore Titanium Silicate Isomorphous to MCM-41 and Its Application as a Catalyst for Selective Oxidation of Hydrocarbons," *J. Chem. Soc., Chem. Commun.*, **1994**, 147–148 (1994).
- Deruane, E.G., "Factors Affecting the Deactivation of Zeolites by Coking," *Stud. Surf. Sci. Catal.*, **20**, 221–239 (1985).
- Fasi, A., I. Palinko, T. Katona, and M. Bartok, "Transformations of Cyclohexene over Silica-Supported Copper in the Presence of Deuterium," *J. Catal.*, **167**, 215–223 (1997).
- Gregg, S.J. and K.S.W. Sing, *Adsorption, Surface Area and Porosity*, Academic Press, London (1982).
- Hunka, D.E., T. Picciotto, D.M. Jaramillo, and D.P. Land, "Dehydrogenation of Cyclohexene to Benzene on Pd (111)," *Surf. Sci.*, **421**, L166–L170 (1999).
- Karge, H.G., J.P. Lange, A. Gutsze, and M. Laniecki, "Coke Formation through the Reaction of Olefins over Hydrogen Mordenite. II. In Situ EPR Measurements under On-Stream Conditions," *J. Catal.*, **114**, 144–152 (1988).
- Kresge, C.T., M.E. Leonowicz, W.J. Roth, J.C. Vartuli, and J.S. Beck, "Ordered Mesoporous Molecular Sieves Synthesized by Liquid-Crystal Templating Mechanism," *Nature*, **359**, 710–712 (1992).
- Kruk, M., M. Jaroniec, and A. Sayari, "Application of Large Pore MCM-41 Molecular Sieves To Improve Pore Size Analysis Using Nitrogen Adsorption Measurements," *Langmuir*, **13**, 6267–6273 (1997).
- Lezanska, M., *Characteristics of mesoporous molecular sieves modified by coking* (Polish), Doctor's Thesis, Nicolaus Copernicus University, Torun, Poland, 2002.
- Llewellyn, P.L., F. Schueth, Y. Grillet, F. Rouquerol, J. Rouquerol, and K.K. Unger, "Water Sorption on Mesoporous Aluminosilicate MCM-41," *Langmuir*, **11**, 574–577 (1995).
- Maglara, E., R. Kaminski, and W. C. Conner, "Analysis of HRADS Adsorption," in *Characterisation of Porous Solids*, B. McEnaney, T.J. Mays, J. Rouquerol, F. Rodrigues-Reinoso, K.S.W. Sing, and K.K. Unger (Eds.), pp. 25–32, Royal Society of Chemistry, London, 1997.
- Navio, J.A., G. Colon, M. Macias, J.M. Campelo, A.A. Romero, and J.M. Marinas, "Catalytic Properties of ZrO₂-SiO₂: Effects of Sulfation in the Cyclohexene Isomerization Reaction," *J. Catal.*, **161**, 605–613 (1996).
- Navio, J.A., G. Colon, M. Macias, J.M. Campelo, A.A. Romero, and J.M. Marinas, "Catalytic Properties of Sulfated and Non-sulfated ZrO₂-SiO₂: Effects of the Sulfation Submitted Before or After the Calcination Process, in the Cyclohexene Isomerization Reaction," *J. Mol. Catal. A.*, **135**, 155–162 (1998).
- Novakova, J. and L. Kubelkova, "Coke Oxidation in ZSM-5 Zeolites. Intermediates, Final Products and Reformation of OH Groups and Void Volumes," *Stud. Surf. Sci. Catal.*, **65**, 405–414 (1991).
- Nowak, L., M. Lezanska, M. Rozwadowski, F. Rozploch, and W. Marciniak, "EPR Studies of Carbonaceous Compounds Deposited on Al-MCM-41," *Appl. Surf. Sci.*, **201**, 182–190 (2002).
- Radwan, N.R.E. and M.M. Selim, "Conversion of Cyclohexene over Y-Zeolite Containing Different Ions," *Bull. Soc. Chim. Belg.*, **105**, 747–753 (1996).
- Reddy, K.M., I.L. Moudrakovski, and A. Sayari, "Synthesis of Mesoporous Vanadium Silicate Molecular Sieves," *J. Chem. Soc., Chem. Commun.*, **1994**, 1059–1060 (1994).
- Rozwadowski, M., J. Wloch, K. Erdmann, and J. Kornatowski, "Influence of the Degree of Ion Exchange on the Sorption Properties of Coked Zeolite Y," *Bull. Soc. Chim. Belg.*, **101**, 463–472 (1992a).
- Rozwadowski, M., J. Wloch, K. Erdmann, and J. Kornatowski, "Sorption Properties of Zeolite Y Modified by Controlled Deposition of Intracrystalline Coke," *Collect. Czech. Chem. Commun.*, **57**, 959–968 (1992b).
- Rozwadowski, M., J. Wloch, J. Kornatowski, M. Pruski, and D. Lang, "Spectroscopic Studies of Carbonaceous Inorganic Adsorbents Prepared from Zeolite Y by Controlled Deposition of Coke in the Process of Methanol Conversion," in *Proceedings of the Polish Chemical Society Symposium on Characterization and Properties of Zeolitic Materials*, M. Rozwadowski (Ed.), pp. 89–100, Nicolaus Copernicus University Press, Torun, Poland, 1994.
- Rozwadowski, M., M. Lezanska, J. Wloch, K. Erdmann, R. Golembiewski, and J. Kornatowski, "Al-MCM-41 Modified by Carbonaceous Deposits: Characterisation by Nitrogen Adsorption Measurements," *Phys. Chem. Chem. Phys.*, **2**, 5510–5516 (2000).
- Rozwadowski, M., M. Lezanska, J. Wloch, K. Erdmann, R. Golembiewski, and J. Kornatowski, "Investigation of Coke Deposits on Al-MCM-41," *Chem. Mater.*, **13**, 1609–1616 (2001a).
- Rozwadowski, M., J. Datka, M. Lezanska, J. Wloch, K. Erdmann, and J. Kornatowski, "Al-MCM-41: Its Acidity and Activity in

- Cyclohexene Conversion," *Phys. Chem. Chem. Phys.*, **3**, 5082–5086 (2001b).
- Rozwadowski, M., M. Lezanska, J. Wloch, K. Erdmann, R. Golembiewski, and J. Kornatowski, "Mechanism of Adsorption of Water, Benzene and Nitrogen on Al-MCM-41 and Effect of Coking on the Adsorption," *Langmuir*, **17**, 2112–2119 (2001c).
- Rozwadowski, M., M. Lezanska, J. Wloch, K. Erdmann, G. Zadrozna, and J. Kornatowski, "Volatile Products of the Conversion of Cyclohexene over Al-MCM-41," *Stud. Surf. Sci. Catal.*, **135**, 4207–4214 (2001d).
- Sayari, A., C. Danumah, and I.L. Moudrakovski, "Boron-Modified MCM-41 Mesoporous Molecular Sieves," *Chem. Mater.*, **7**, 813–815 (1995a).
- Sayari, A., I.L. Moudrakovski, C. Danumah, C.I. Ratcliffe, J.A. Ripmeester, and K. F. Preston, "Synthesis and NMR Study of Boron-Modified MCM-41 Mesoporous Materials," *J. Phys. Chem.*, **99**, 16373–16379 (1995b).
- Sayari, A., K.M. Reddy, and I. Moudrakovski, "Synthesis of V and Ti modified MCM-41 Mesoporous Molecular Sieves," *Stud. Surf. Sci. Catal.*, **98**, 19–21 (1995c).
- Sayari, A., "Periodic Mesoporous Materials: Synthesis, Characterization and Potential Applications," *Stud. Surf. Sci. Catal.*, **102**, 1–46 (1996).
- Sayari, A., P. Liu, M. Kruk, and M. Jaroniec, "Characterization of Large Pore MCM-41 Molecular Sieves Obtained via Hydrothermal Restructuring," *Chem. Mater.*, **9**, 2499–2506 (1997).
- Tanev, P.T., M. Chibwe, and T.J. Pinnavaia, "Titanium-Containing Mesoporous Molecular Sieves for Catalytic Oxidation of Aromatic Compounds," *Nature*, **368**, 321–323 (1994).
- Weglarski, J., J. Datka, H. He, and J. Klinowski, "IR Spectroscopic Studies of the Acidic Properties of the Mesoporous Molecular Sieve MCM-41," *J. Chem. Soc., Faraday Trans.*, **92**, 5161–5164 (1996).
- Weitkamp, J., S. Ernst, H. Dauns, and E. Gallei, "Shape-Selective Catalysis in Zeolites," *Chem. Ing. Techn.*, **58**, 623–632 (1986).
- Wloch, J., M. Rozwadowski, K. Erdmann, and J. Bludzinska, "Investigation of Coke Deposits on Zeolite HNaY," in *Proceedings of the 2nd Polish-German Zeolite Colloquium*, M. Rozwadowski (Ed.), pp. 141–152, Nicolaus Copernicus University Press, Torun, Poland, 1995.
- Wloch, J., M. Rozwadowski, and K. Erdmann, "Carbon-Zeolite Porous Materials. I. Preparation and Investigation of Coke Deposits," in *Proceedings of the 3rd Polish-German Zeolite Colloquium*, M. Rozwadowski (Ed.), pp. 255–270, Nicolaus Copernicus University Press, Torun, Poland, 1998a.
- Wloch, J., M. Rozwadowski, K. Erdmann, and R. Golembiewski, "Carbon-Zeolite Porous Materials. II. Adsorption and Catalytic Properties," in *Proceedings of the 3rd Polish-German Zeolite Colloquium*, M. Rozwadowski (Ed.), pp. 271–283, Nicolaus Copernicus University Press, Torun, Poland, 1998b.